Anisotropic Nature of Anatase TiO_2 and Its Intrinsic (001) Surface Electronic States

Hungru Chen,[1,*] James A. Dawson,[2] and Naoto Umezawa[1,†]

[1]*Environmental Remediation Materials Unit, National Institute for Materials Sciences, Ibaraki 305-0044, Japan*

[2]*Department of Materials Science and Engineering, Kyoto University, Sakyo, Kyoto 606-8501, Japan*

(Received 22 October 2014; revised manuscript received 6 February 2015; published 20 July 2015)

Anatase TiO_2 attracts considerable interest for a range of technological applications such as photocatalysis and electronic memory devices. Recent studies have shown that the (001) surface plays a crucial role in its photocatalytic activity and this has been attributed to its higher surface energy and its ability to adsorb water dissociatively. However, a fundamental understanding of why this surface is so unique is still lacking. In this study, the anatase TiO_2 (001) and (101) surfaces, both present in its equilibrium crystal shape, are studied using state-of-the-art *ab initio* hybrid density-functional-theory calculations. It is found that the electronic states at the (001) surface strongly deviate from the bulk, while the electronic states at the (101) surface do not. We illustrate the role of anisotropy in the crystal on the electronic structures of anatase TiO_2 and demonstrate how the formation of the (001) surface disrupts local orbital interactions and gives rise to distinctive surface electronic states, which give the (001) surface its unique properties.

DOI: 10.1103/PhysRevApplied.4.014007

I. INTRODUCTION

Many of the functionalities of metal oxides come from surface-related phenomena and therefore are largely determined by surface rather than bulk properties. A fundamental understanding of the surface electronic structure of metal oxides is essential in order to advance fields such as catalysis and electrochemistry on metal oxide surfaces. Because of the change in electrostatic (Madelung) potential and the reduction of local coordination, the electronic structure at the surface of a metal oxide can be very different from that of the bulk material [1–3]. The presence of surface states with localized character, either extending into or entirely residing inside the bulk band gap has been predicted and it can have a significant effect on molecule adsorption [4,5]. Nevertheless, only a few metal oxides actually exhibit distinctive "intrinsic" surface states, while most observed surface states of metal oxides originate from surface defects and are hence deemed "extrinsic" [6–8].

Titanium dioxide (TiO_2) is one of the most studied materials in photocatalysis [9] and also finds applications in many other technologies including solar cells [10] and electronic memory devices [11]. Two common polymorphs of TiO_2 are anatase and rutile. The anatase phase is generally found to be more photocatalytically active than the rutile phase for reasons that are not yet clear [12,13]. As a result, the anatase TiO_2 has been subjected to intensive studies in order to further improve its activity. Recently, the ratio of exposed (001) surface on anatase TiO_2 crystal has been shown to have a positive correlation with its photocatalytic activity [14,15] as well as the efficiency of dye-sensitized solar cells [16,17]. Although there exist several theoretical works on anatase TiO_2 surfaces [18–21], most of them concern energetics and adsorptions, whereas the surface electronic structures have not been discussed thoroughly. Most importantly, there is no fundamental understanding why the anatase TiO_2 (001) surface is different from other surfaces.

In this work, the electronic structure of the two surfaces appearing in the equilibrium crystal shape of anatase TiO_2, the (001) and (101) surfaces [18], are investigated by theoretical *ab initio* calculations. We discover intrinsic surface electronic states at the (001) surface that extend into the bulk band gap, which in effect raises the band-edge position. In contrast, the (101) surface band-edge position remains unchanged relative to the bulk. Detailed analysis of orbital interactions reveals that this can be attributed to the anisotropic nature of anatase TiO_2.

II. METHODS

All calculations are based on density functional theory and we utilize the range-separated screened hybrid functional HSE06 [22], which mixes 25% Hartree-Fock exchange with 75% generalized-gradient-approximation–Perdew-Burke-Ernzerhof functional, as implemented in the Vienna *ab initio* simulation package (VASP) [23]. Valence electrons are described by a plane-wave basis set with an energy cutoff of 400 eV. The interactions between core and valence electrons are treated with the projector-augmented-wave method [24].

*Present address: Department of Chemistry, University of Bath, Bath BA2 7AY, United Kingdom.
h.chen@bath.ac.uk

†umezawa.naoto@nims.go.jp

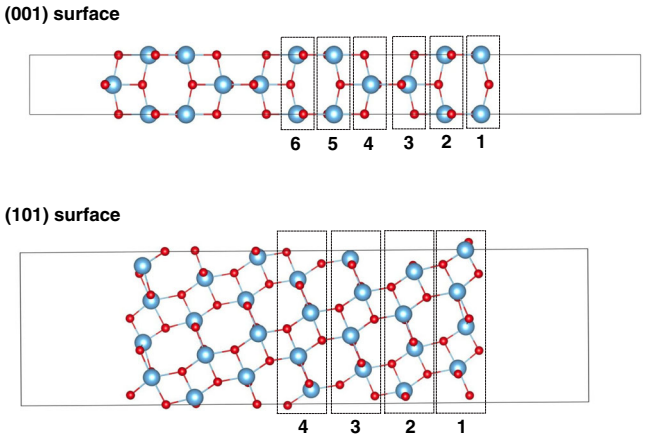

FIG. 1. Structural models for the anatase TiO_2 (001) and (101) surfaces. TiO_2 layers are labeled numerically. The blue and red spheres denote titanium and oxygen ions, respectively.

The anatase TiO_2 (001) and (101) surfaces are modeled using periodic slabs with thicknesses over 23 Å as shown in Fig. 1, so that the ions deep in the middle of the slab represent the bulk. The repeated slabs in the z direction are separated by a ~15-Å-wide vacuum region. The k space is sampled with a gamma-point-centered $10 \times 10 \times 1$ mesh for the (001) surface cell and a $3 \times 8 \times 1$ mesh for the (101) surface cell. Atomic positions are optimized until the force is converged to less than 0.03 eV $Å^{-1}$.

It is know that the (001) surface undergoes a (1×4) reconstruction under ultrahigh vacuum on epitaxially grown thin films at high temperature [25,26]. Nonetheless, the positive correlation between the exposed (001) surface and activities is observed only in micro- and nanocrystalline samples, synthesized by solution-based methods [27,28]. It is not clear whether the (001) surface reconstruction also occurs in these micro- and nanosized anatase crystals. In fact, the equilibrium crystal shape predicted using the calculated surface energy of the unconstructed (001) surface is consistent with the naturally occurring and nanocrystalline anatase synthesized under neutral aqueous conditions [18]. The (001) surface makes only a small fraction of the entire exposed surface due to its high surface energy. Besides, a recent experiment actually shows that the (1×4) reconstruction on epitaxially grown anatase thin film deactivates the (001) surface toward water adsorption [29]. Therefore, in this study only the unreconstructed (1×1) (001) surface is considered.

III. RESULTS AND DISCUSSION

Figure 2 shows the layer-resolved density of states (DOS) for the anatase TiO_2 (001) and (101) surfaces. In the anatase structure, each oxygen anion (O^{2-}) is coordinated by or bonded to three titanium cations (Ti^{4+}) forming T-shape-like Ti_3O units. We define p_σ as the oxygen-$2p$ orbital whose lobes point toward Ti ions on each side in the basal plane, p_π as the $2p$ orbital whose lobes point out of the Ti_3O plane and p_z as the $2p$ orbital with only one lobe pointing towards Ti ions out of the basal plane in the z direction. Because of the attractive Coulomb force, the oxygen $2p$ electrons closer to positively charged Ti^{4+} cations have lower energy. Therefore, the three oxygen $2p$ levels are split by the crystal field, resulting in the p_σ orbital being the lowest in energy and the p_π orbital being the highest, as clearly shown by the calculated oxygen DOS in Fig. 2.

It is clear that the (001) surface exhibits a distinctive electronic structure that is different from the bulk. Specifically, the electronic states from the twofold-coordinated oxygen ions (O_{2c}) at the (001) surface extend into the bulk band gap with a predominately localized p_π character, resulting in the highest occupied energy level being 0.8 eV higher than the oxygen deep in the bulk [O (6) in the DOS plot]. This behavior has also been observed in a previous theoretical work [19]. These surface states are "intrinsic" as they do not result from surface impurities or defects. Since the valence-band top of TiO_2 is predominately composed of oxygen $2p$ states, it can be derived that the

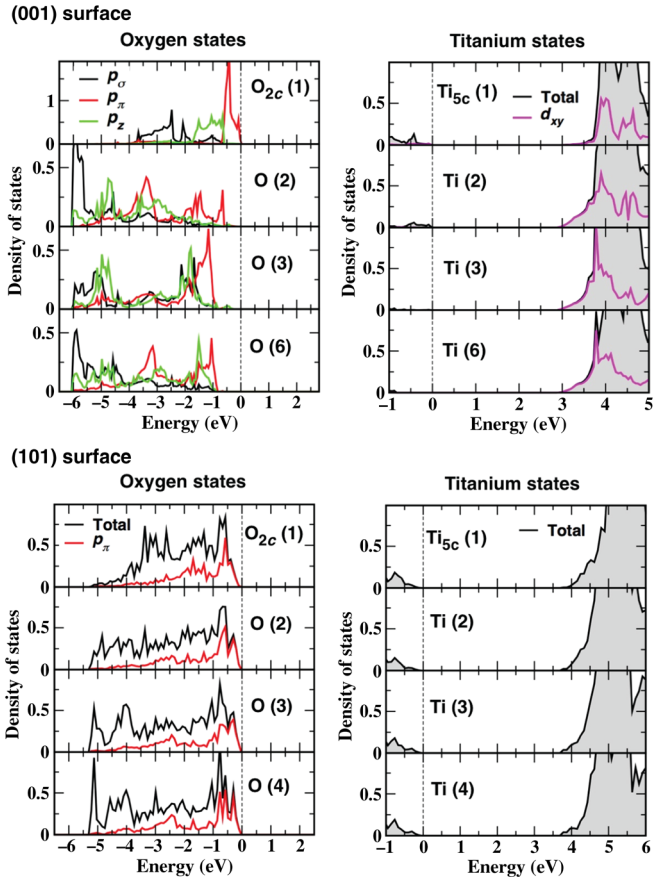

FIG. 2. Layer-decomposed density of states. The layer number is indicated in parentheses, which increases from surface to bulk. The Fermi level is aligned to 0 eV and is indicated by the dashed line.

valence-band maximum (VBM) at the (001) surface is 0.8 eV higher than in the bulk. Also, from the layer-decomposed Ti DOS, the conduction-band minimum (CBM) at the (001) surface is about 0.2 eV higher than in the bulk. On the other hand, there is no noticeable shift of the VBM and CBM positions at the (101) surface.

The unique electronic structure at the (001) surface has the following consequences. First, the high-lying electronic energy levels associated with surface oxygen ions contribute directly to the higher (001) surface energy compared to the (101) surface. Second, surface states with localized character inside the bulk band gap have been suggested to favor molecular adsorption because these states can be more easily transferred and shared, whereas diffuse surface states cannot interact efficiently with adsorbates [4]. This is supported by previous calculations showing better molecular adsorption on the (001) surface [19]. Third, the presence of the (001) surface electronic states inside the bulk band gap reduces the (001) surface band gap. The smaller band gap extends the light absorption toward the visible region, which is beneficial for solar-energy conversion applications such as photocatalysis and solar cells. Indeed, experiments have shown better light absorption when the percentage of exposed (001) surface is higher [15,30]. Fourth, the higher positions of VBM as shown in Fig. 3 and the localized character of oxygen p states shown in Fig. 2 indicate the (001) surface a strong hole-trapping location, whereas the higher CBM position will repel electrons. The coexistence of the (101) and (001) surfaces can therefore have a charge separation effect, as shown in Fig. 3. This is in agreement with recent experimental studies that directly observe preferential hole trapping on the (001) surface and electron trapping at the (101) surface [31,32]. In addition, higher efficiency of dye-sensitized anatase TiO_2 solar cells with an increased percentage of exposed (001) surface can also be explained by the higher position of CBM at the (001) surface. Once an electron is injected in TiO_2 through the (001) surface, the higher CBM position will then prevent the back-electron transfer from the conduction band to dye and hence suppress the recombination.

Now the question is why the (001) surface exhibits such a different electronic structure while the (101) surface does not. The surface electronic structure of ionic crystals can deviate from the bulk due to different electrostatic potentials, reduced coordination numbers, and orbital interactions, leading to smaller bandwidths at the surface [1,2]. Figure 4 shows the calculated on-site electrostatic potential [33] of titanium and oxygen ions at different depths below the (001) and (101) surfaces. First, if vacuum is used as the common reference, there would be a 1.2 eV offset in the bulk potential between (001) and (101) surfaces, which indicates that the (101) surface work function is 1.2 eV larger than the (001) surface. Next, it is shown that at the (001) surface, the twofold-coordinated oxygen on-site electrostatic potential rises substantially by 1.2 eV compared to the bulk oxygen. Also, the electrostatic potential at the surface fivefold-coordinated titanium site is about 0.2 eV higher than the bulk titanium. These values agree well with the upshift of VBM and CBM at the (001) surface. In contrast, while there is a 0.3 eV rise of electrostatic potential at the (101) surface fivefold-coordinated titanium site, there is no change at the (101) surface oxygen site.

Apart from the shift of the VBM and CBM positions, there is another important feature in the layer-resolved DOS of the (001) surface that has not been discussed so far. As shown in Fig. 2, the overall oxygen $2p$ band in the bulk has a width of about 5.3 eV, but is narrowed to less than 4 eV at the (001) surface. The narrowing of the p_π and p_z widths of the (001) surface oxygen O_{2c} is particularly significant. These indicate reduced orbital interactions at the (001) surface. To understand the orbital interactions in anatase TiO_2, we look at its bulk electronic structure. Figure 5(a) shows the crystal structure of anatase TiO_2 and Fig. 5(b) shows the calculated anatase TiO_2 band structure for the conventional body-centered-tetragonal unit cell. It is shown that all bands are dispersive in the basal plane

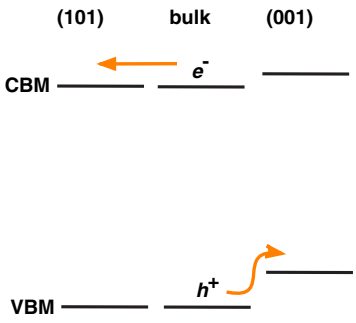

FIG. 3. Band-edge positions at the (101) and (001) surfaces relative to the bulk.

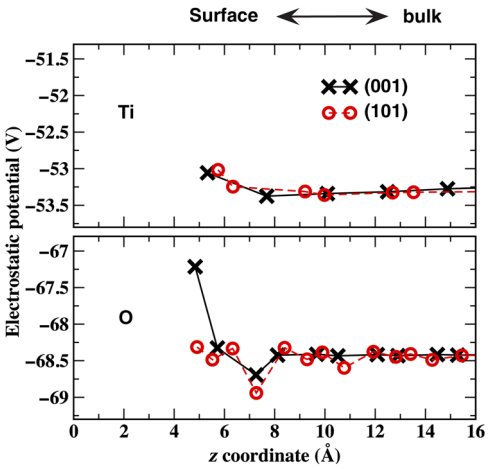

FIG. 4. Calculated on-site electrostatic potential at titanium and oxygen sites against the depth for the (001) and (101) surfaces. Note that the potentials of the two cells in the bulk region are aligned and vaccum is not the common reference.

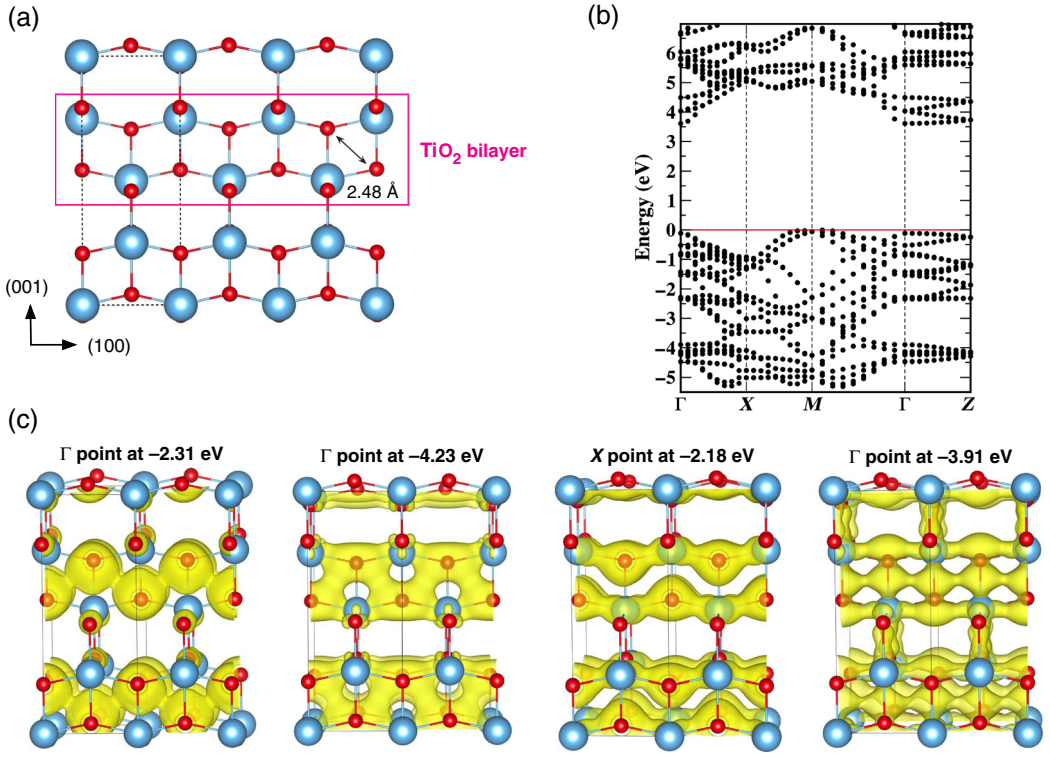

FIG. 5 (a) Crystal structure of anatase TiO_2. The conventional unit cell is indicated by a dashed line. (b) Band structure of bulk anatase TiO_2. (c) Partial charge densities showing bonding characters at four specified points in the band structure. The isosurfaces shown correspond to a density of 2.5–07 e Å^3.

($\Gamma \rightarrow X \rightarrow M \rightarrow \Gamma$), but nearly flat along the (001) direction ($\Gamma \rightarrow Z$), which means that stronger orbital interactions exist in the basal plane, whereas weaker interactions occur along the Z direction. This two-dimensional character is reflected in experimentally measured large electron mass anisotropy [34].

Figure 5(c) shows partial charge densities at four different selected points in the band structure. The charge density at the Γ point at -2.31 eV shows a direct p_π-p_π bonding interaction between nearest-neighboring oxygen ions along the zigzag chains. The charge density at the Γ point at -4.23 eV shows a direct p_σ-p_σ bonding interaction between nearest-neighboring oxygen ions. The charge density at the X point at -2.18 eV shows a p_π-d_{xy}-p_π bonding interaction between oxygen and titanium ions. The charge density at the Γ point at -3.91 eV shows a direct p_z-p_z bonding interaction between nearest-neighboring oxygen ions as well as a p_z-d_{z^2}-p_z bonding interaction between oxygen and titanium ions. These orbital interactions run through the TiO_2 bilayer and give rise to band dispersion in the basal plane. No interaction is seen along the (001) direction, in agreement with flat bands along the $\Gamma \rightarrow Z$ direction in the band structure. These anisotropic orbital interactions originate from the crystal structure of the anatase TiO_2. As shown in Fig. 5(a), in the anatase structure, nearest-neighboring oxygen ions form zigzag chains along the (100) and (010) directions. The distance between nearest-neighboring oxygen ions is unusually short, only 2.48 Å, due to strongly distorted TiO_6 octahedra. This short distance consequently enhances the strength of direct oxygen-oxygen orbital interactions within the TiO_2 bilayers.

Now we can explain the different electronic structures between the anatase (001) and (101) surfaces. Figure 6 shows that when the (001) surface is formed, the twofold-coordinated oxygen ions O_{2c} at the surface lose

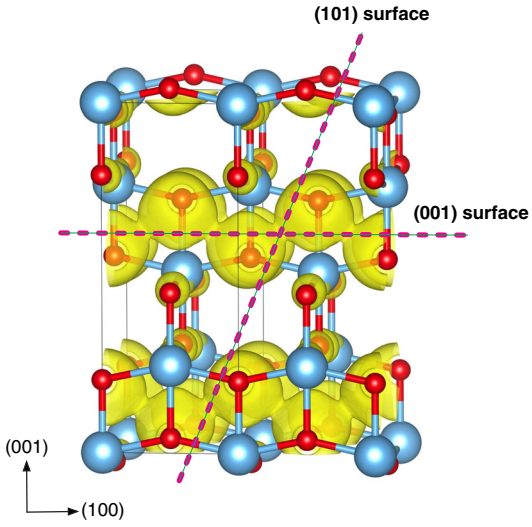

FIG. 6. Illustration of the (001) and (101) surface cuts.

their nearest-neighboring oxygen ions. This means that the direct oxygen p orbital interactions along the zigzag chain, that give rise to the dispersion of the oxygen p electronic states, no longer exist. Also, surface twofold-coordinated oxygen ions O_{2c} only couple weakly with oxygen ions below the (001) surface due to insignificant orbital interactions along the (001) direction as discussed above. Consequently, the p_σ, p_π, and p_z states of the surface twofold-coordinated oxygen ions O_{2c} are not only raised in energy by the increased electrostatic potential at the surface, but also become narrowed and localized, as seen in the layer-resolved DOS in Fig. 2. Similarly, the Ti d_{xy} state, of which the bottom of anatase TiO_2 conduction is mainly composed [35], at the (001) surface is narrowed due to reduced orbital interactions and the upshift of CBM results.

In contrast to the (001) surface, the ions at the (101) surface can still interact substantially with ions below the surface along the (100) and (010) directions. Through these interactions, the electronic states at the (101) surface remain dispersive and stabilized despite the increased electrostatic potential. In other words, the electronic states at the (101) surface couple strongly to bulk electronic states and can be regarded as just the extension of bulk electronic states and hence can be deemed "surface resonances" [36].

IV. CONCLUSIONS

In summary, it has been demonstrated that the (001) surface exhibits a distinctive intrinsic surface electronic structure that is different from the bulk while the (101) surface does not. The upshift of VBM and CBM positions at the (001) surface should attract holes but repel electrons, in agreement with experiment. Therefore, the existence of the (001) surface in the equilibrium shape of anatase [14] can always facilitate electron-hole charge separation. We suggest this is the reason why nanocrystalline anatase is more photocatalytically active than rutile.

Moreover, the underlying physical mechanism that is responsible for the difference between the two considered surfaces is identified. It is noticed that the orbital interactions and dispersions in anatase TiO_2 are two dimensional owing to its crystal anisotropy, that is, interactions are strong within TiO_2 bilayers parallel to the basal plane but weak along the (001) direction. Consequently, due to the raised electrostatic potential and reduced bilayer orbital interactions, the (001) surface states exhibit localized character and extend inside the bulk band gap. On the other hand, the (101) surface couples strongly with bulk through the (010) direction and can be regarded as an extension of bulk states.

The fundamental understanding of surface electronic structure acquired in this study provides a direction in the search and engineering of new materials, especially for surface-related applications such as catalysis, photocatalyisis, and dye-sensitized solar cells. As demonstrated in this study, anisotropy in crystal structures is likely to cause reduced orbital interaction at a low-index surface and, consequently, localized surface states inside the bulk band gap. These surface states can then play an important role in molecular adsorption, charge dynamics, interfacial charge transfer, and optical properties.

ACKNOWLEDGMENTS

H. C. thanks K. T. Butler for helpful discussions. This work is partly supported by the Japan Science and Technology Agency (JST) Precursory Research for Embryonic Science and Technology (PRESTO) program.

[1] V. E. Heinrich and P. A. Cox, *The Surface Science of Metal Oxides* (Cambridge University Press, New York, 1994).
[2] C. Noguera, *Physics and Chemistry at Oxide Surfaces* (Cambridge University Press, New York, 1996).
[3] M. Tsukada, H. Adachi, and C. Satoko, Theory of electronic structure of oxide surfaces, Prog. Surf. Sci. **14**, 113 (1983).
[4] F. J. Morin and T. Wolfram, Surface States and Catalysis on *d*-Band Perovskite, Phys. Rev. Lett. **30**, 1214 (1973).
[5] T. Wolfram, E. A. Kraut, and F. J. Morin, *d*-band surface state on transition-metal perovskite crystals: I. Qualitative features and application to $SrTiO_3$, Phys. Rev. B **7**, 1677 (1973).
[6] V. E. Henrich, G. Dresselhaus, and H. J. Zeiger, Energy-dependent electron-energy-loss spectroscopy: Application to the surface and bulk electronic structure of MgO, Phys. Rev. B **22**, 4764 (1980).
[7] V. E. Henrich, G. Dresselhaus, and H. J. Zeiger, Surface defects and the electronic structure of $SrTiO_3$ surfaces, Phys. Rev. B **17**, 4908 (1978).
[8] V. E. Henrich and R. L. Kurtz, Surface electronic structure of TiO_2: Atomic geometry, ligand coordination, and the effect of adsorbed hydrogen, Phys. Rev. B **23**, 6280 (1981).
[9] A. L. Linsebigler, G. Lu, and J. T. Yates, Photocatalysis on TiO_2 surfaces: Principles, mechanisms, and selected results, Chem. Rev. **95**, 735 (1995).
[10] U. Bach, D. Lupo, P. Comte, J. E. Moser, F. Weissortel, J. Salbeck, H. Spreitzer, and M. Gratzel, Solid-state dye-sensitized mesoporous TiO_2 solar cells with high photon-to-electron conversion efficiencies, Nature (London) **395**, 583 (1998).
[11] D.-H. Kwon *et al.*, Atomic structure of conducting nanofilaments in TiO_2 resistive switching memory, Nat. Nanotechnol. **5**, 148 (2010).
[12] A. Sclafani and J. M. Herrmann, Comparison of the photoelectronic and photocatalytic activities of various anatase and rutile forms of titania in pure liquid organic phase and in aqueous solutions, J. Phys. Chem. **100**, 13655 (1996).
[13] T. Luttrell, S. Halpegamage, J. Tao, A. Kramer, E. Sutter, and M. Batzill, Why is anatase a better photocatalyst than rutile?—Model studies on expitaxial TiO_2 films, Sci. Rep. **4**, 4043 (2014).
[14] J. Yu, J. Low, W. Xiao, P. Zhou, and M. Jaroniec, Enhanced photocatalytic-CO_2 reduction activity of anatase TiO_2 by coexposed {001} and {101} facets, J. Am. Chem. Soc. **136**, 8839 (2014).

[15] J. Pan, G. Liu, G. Q. Lu, and H.-M. Cheng, On the true photoreactivity order of {001}, {010}, and {101} facets of anatase TiO_2 crystals, Angew. Chem., Int. Ed. **50**, 2133 (2011).

[16] X. Wu, Z. Chen, G. Q. Lu, and L. Wang, Nanosized anatase TiO_2 single crystals with tunable exposed (001) facets for enhanced energy conversion efficiency of dye-sensitized solar cells, Adv. Funct. Mater. **21**, 4167 (2011).

[17] F. Hao, X. Wang, C. Zhou, X. Jiao, X. Li, J. Li, and H. Lin, Efficient light harvesting and charge collection of dye-sensitized solar cells with (001) faceted single crystalline anatase nanoparticles, J. Phys. Chem. C **116**, 19164 (2012).

[18] M. Lazzeri, A. Vittadini, and A. Selloni, Structure and energetics of stoichiometric TiO_2 anatase surfaces, Phys. Rev. B **63**, 155409 (2001).

[19] X.-Q. Gong and A. Selloni, Reactivity of anatase TiO_2 nanoparticles: The role of the minority (001) surface, J. Phys. Chem. B **109**, 19560 (2005).

[20] A. Vittadini, A. Selloni, F. P. Rotzinger, and M. Grätzel, Structure and Energetics of Water Adsorbed at TiO_2 Anatase 101 and 001 Surfaces, Phys. Rev. Lett. **81**, 2954 (1998).

[21] Z. Zongyan, L. Zhaosheng, and Z. Zhigang, Surface properties and electronic structure of low-index stoichiometric anatase TiO_2 surfaces, J. Phys. Condens. Matter **22**, 175008 (2010).

[22] A. V. Krukau, O. A. Vydrov, A. F. Izmaylov, and G. E. Scuseria, Influence of the exchanges screening parameter on the performance of screened hybrid functionals, J. Chem. Phys. **125**, 224106 (2006).

[23] G. Kresse and J. Furthmüller, Efficient iterative schemes for *ab initio* total-energy calculations using a plane-wave basis set, Phys. Rev. B **54**, 11169 (1996).

[24] P. E. Blöchl, Projector augmented-wave method, Phys. Rev. B **50**, 17953 (1994).

[25] G. S. Herman, M. R. Sievers, and Y. Gao, Structure Determination of the Two-Domain (1×4) Anatase TiO_2 (001) Surface, Phys. Rev. Lett. **84**, 3354 (2000).

[26] Y. Du, D. J. Kim, T. C. Kaspar, S. E. Chamberlin, I. Lyubinetsky, and S. A. Chambers, *In-situ* imaging of the nucleation and growth of epitaxial anatase, Surf. Sci. **606**, 1443 (2012).

[27] H. G. Yang, C. H. Sun, S. Z. Qiao, J. Zou, G. Liu, S. C. Smith, H. M. Cheng, and G. Q. Lu, Anatase TiO_2 single crystals with a large percentage of reactive facets, Nature (London) **453**, 638 (2008).

[28] X.-L. Cheng, M. Hu, R. Huang, and J.-S. Jiang, HF-free synthesis of anatase TiO_2 nanosheets with largely exposed and clean {001} facets and their enhanced rate performance as anodes of lithium-ion battery, ACS Appl. Mater. Interfaces **6**, 19176 (2014).

[29] Y. Wang *et al.*, Role of point defects on the reactivity of reconstructed anatase titanium dioxide (001) surface, Nat. Commun. **4**, 2214 (2013).

[30] G. Liu, C. Sun, H. G. Yang, S. C. Smith, L. Wang, G. Q. Lu, and H.-M. Cheng, Nanosized anatase TiO_2 single crystals for enhanced photocatalytic activity, Chem. Commun. (Cambridge) **46**, 755 (2010).

[31] M. D'Arienzo, J. Carbajo, A. Bahamonde, M. Crippa, S. Polizzi, R. Scotti, L. Wahba, and F. Morazzoni, Photogenerated defects in shape-controlled TiO_2 anatase nanocrystals: A probe to evaluate the role of crystal facets in photocatalytic processes, J. Am. Chem. Soc. **133**, 17652 (2011).

[32] T. Tachikawa, S. Yamashita,, and T. Majima, Evidence for crystal-face-depedent TiO_2 photocatalysis from single-molecule imaging and kinetics analysis, J. Am. Chem. Soc. **133**, 7197 (2011).

[33] The on-site electrostatic potential is calculated by integrating the electrostatic potential V with a test charge ρ from an ionic position R over a spatial extension $\bar{V} = \int V(r)\rho(|r - R|)d^3r$.

[34] Y. Hirose, N. Yamada, S. Nakao, T. Hitosugi, T. Shimada, and T. Hasegawa, Large electron mass anisotropy in a *d*-electron-based transparent conducting oxide: Nb-doped anatase TiO_2 epitaxial films, Phys. Rev. B **79**, 165108 (2009).

[35] R. Asahi, Y. Taga, W. Mannstadt, and A. J. Freeman, Electronic and optical properties of anatase TiO_2, Phys. Rev. B **61**, 7459 (2000).

[36] P. Y. Yu and M. Cardona, *Fundamentals of Semiconductors—Physics and Materials Properties* (Springer, New York, 1996).